Nicolas V. Jaumard
e-mail: njaumard@mail.med.upenn.edu

Joel A. Bauman

Dept. of Neurosurgery,
University of Pennsylvania,
HUP-3 Silverstein,
3400 Spruce Street,
Philadelphia, PA 19104

Christine L. Weisshaar
Dept. of Neurosurgery,
University of Pennsylvania,
HUP-3 Silverstein,
3400 Spruce Street,
Philadelphia, PA 19104;
Dept. of Bioengineering,
University of Pennsylvania,
210 S. 33rd Street,
Room 240 Skirkanich Hall,
Philadelphia, PA 19104

Benjamin B. Guarino
Dept. of Bioengineering,
University of Pennsylvania,
210 S. 33rd Street,
Room 240 Skirkanich Hall,
Philadelphia, PA 19104

William C. Welch
Dept. of Neurosurgery,
University of Pennsylvania,
HUP-3 Silverstein,
3400 Spruce Street,
Philadelphia, PA 19104

Beth A. Winkelstein[1]
Dept. of Neurosurgery,
University of Pennsylvania,
HUP-3 Silverstein,
3400 Spruce Street,
Philadelphia, PA 19104;
Dept. of Bioengineering,
University of Pennsylvania,
210 S. 33rd Street,
Room 240 Skirkanich Hall,
Philadelphia, PA 19104
e-mail: winkelst@seas.upenn.edu

Contact Pressure in the Facet Joint During Sagittal Bending of the Cadaveric Cervical Spine

The facet joint contributes to the normal biomechanical function of the spine by transmitting loads and limiting motions via articular contact. However, little is known about the contact pressure response for this joint. Such information can provide a quantitative measure of the facet joint's local environment. The objective of this study was to measure facet pressure during physiologic bending in the cervical spine, using a joint capsule-sparing technique. Flexion and extension bending moments were applied to six human cadaveric cervical spines. Global motions (C2-T1) were defined using infra-red cameras to track markers on each vertebra. Contact pressure in the C5-C6 facet was also measured using a tip-mounted pressure transducer inserted into the joint space through a hole in the postero-inferior region of the C5 lateral mass. Facet contact pressure increased by 67.6 ± 26.9 kPa under a 2.4 Nm extension moment and decreased by 10.3 ± 9.7 kPa under a 2.7 Nm flexion moment. The mean rotation of the overall cervical specimen motion segments was 9.6 ± 0.8° and was 1.6 ± 0.7° for the C5-C6 joint, respectively, for extension. The change in pressure during extension was linearly related to both the change in moment (51.4 ± 42.6 kPa/Nm) and the change in C5-C6 angle (18.0 ± 108.9 kPa/deg). Contact pressure in the inferior region of the cervical facet joint increases during extension as the articular surfaces come in contact, and decreases in flexion as the joint opens, similar to reports in the lumbar spine despite the difference in facet orientation in those spinal regions. Joint contact pressure is linearly related to both sagittal moment and spinal rotation. Cartilage degeneration and the presence of meniscoids may account for the variation in the pressure profiles measured during physiologic sagittal bending. This study shows that cervical facet contact pressure can be directly measured with minimal disruption to the joint and is the first to provide local pressure values for the cervical joint in a cadaveric model. [DOI: 10.1115/1.4004409]

Keywords: contact pressure, facet joint, cervical spine, sagittal bending, pressure transducer

1 Introduction

Spinal facet joints are di-arthrodial synovial joints that transmit and absorb loads, as well as limit and couple motions [1,2]. In contrast, nonphysiologic loading to the spine can induce a variety of injuries, including facet dislocation, fractures [1,3,4] or capsular and other neck injuries such as whiplash injuries [5–7]. Facet joints that have been injured or surgically treated can have weakened mechanical function that can lead to or contribute to joint instability and pain [7–12]. Biomechanical studies have demonstrated that both simulated traumatic injury and decompressive surgical procedures modify the local kinematics and kinetics of cervical facet joints [5,6,8]. Total disc arthroplasty designs may also substantially alter facet joint loading [13–16]. The mechanical responses of cervical facet joints have been characterized under physiologic and pathologic conditions [5,6,17]. For example, the posterior aspects of the caudal and rostral articular pillars come in contact with each other during extension, while the anterior region of the joint undergoes distraction; these local kinematics can be modified under dynamic and/or coupled loading conditions in the cervical spine that result in increased shear and distraction [5,6,18,19]. However, despite prior studies defining the bony motions and/or capsular ligament responses, there is little definitive data characterizing the mechanical response of the articular surfaces during normal motions or relating those responses to the kinematics and/or kinetics of the cervical spine.

[1]Corresponding author.

Contributed by the Bioengineering Division of ASME for publication in the JOURNAL OF BIOMECHANICAL ENGINEERING. Manuscript received December 22, 2010; final manuscript received June 2, 2011; published online July 13, 2011. Assoc. Editor: Richard E. Debski.

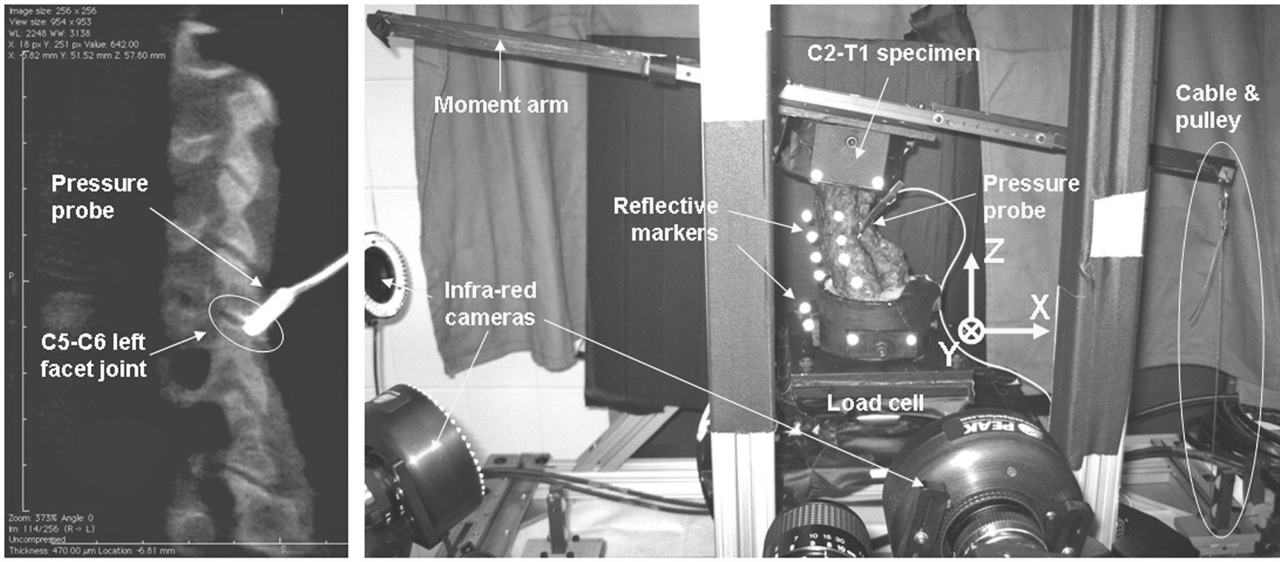

Fig. 1 (*a*) Representative fluoroscopic image of a cadaveric specimen (Specimen #1) showing the pressure probe inserted in the C5-C6 left facet joint. (*b*) Photograph of the test setup showing a cadaveric specimen (Specimen #6) with the pressure probe in the left C5-C6 facet joint, positioned on top of the six-axis load cell. Reflective markers are affixed to the C4-C7 vertebrae and the C2 and T1 cups for motion tracking by the infra-red cameras. The bar serving as a moment arm is attached to the top of the C2 cup and is connected to the cable and pulley system with the specimen oriented for the application of isolated extension.

The facet joint supports between 3 and 32% of the compressive load [20,21] in the cervical spine and up to 25% in the lumbar spine [20,21]. In extension, part of the axial compressive load is carried by the area of the facet articular surfaces that are in contact. As such, contact pressure developing between the articulating bones in the facet joint can define the local loading to that joint. Limited studies have estimated facet force using laminar strain [13,22,23]; other studies have predicted facet contact pressures using finite element models [13,22–26] or inverse kinematic analyses of segmental strains and loading rates [5,6,27]. In the lumbar spine, contact pressures in cadaveric specimens have been measured using flat sensors or films placed directly in the joint space [28–30]. Although those experimental techniques are helpful to estimate the spatial distribution of the maximum contact pressures for a given loading exposure, most of them are not able to provide continuous and/or sub-maximal facet pressure information. Further, directly measuring pressure within the cadaveric joint space typically requires cutting the joint capsular ligament in order to insert any sort of sensor. However, transection of the facet capsule has been shown to induce hypermobility and instability that modify the joint's overall mechanical behavior, and can potentially alter local mechanics and induce nonphysiologic articular contact [9,31]. In addition, the presence of film in a joint space has been shown to overestimate contact areas between articular surfaces and may further alter the joint's mechanical response [32–35]. Despite a growing interest in measuring contact pressures in the facet joint and a variety of technical approaches to do so, there remains a paucity of data defining the contact pressures for even normal physiologic motions and loading using noninvasive methods.

To date, no study has defined the contact pressures during any type of loading scenario for the cervical spine. In fact, only one study in the lumbar spine has investigated facet contact pressures while preserving the facet capsule [36]. In that study, el-Bohy et al. mounted a miniature strain gauge at the end of a stainless steel tube that was affixed in a hole in the inferior region of lumbar articular pillars. Pressure in the lumbar facet joint found to range from 100–300 kPa for an erect posture under a compressive load of 564 ± 80 N combined with a 15 Nm flexion moment [36]. The objective of the present study was to define the facet pressure profiles developed during physiologic sagittal bending in cadaveric cervical spine specimens without violating the mechanical integrity of the facet tissues. Despite the horizontal orientation and mobility of the cervical facets, it was assumed that physiological contact also would occur at the inferior aspect of the facet joint during extension [24,36] and would be smaller in magnitude than in lumbar facet joints. It was further hypothesized that maximal pressure changes would occur at the extreme of the physiologic range of sagittal bending. Using a technique similar to that of el-Bohy et al. [36], a miniature tip-mounted transducer was implemented in a multisegmental human cadaveric cervical spine model to measure C5-C6 facet contact pressures under sagittal bending conditions representative of physiologic facet mechanics.

2 Materials and Methods

A total of six fresh-frozen and thawed male human C2-T1 cadaveric cervical spines ($n = 6$; 59 ± 15 years old) were selected after screening for major bony defects. Tissue procurement and all procedures were approved by the Operational Committee of the University of Pennsylvania School of Medicine; cervical spines were obtained from MedCure Inc. (Portland, OR). Using radiographic images generated by three-dimensional fluoroscopic imaging, a neurosurgeon evaluated the degree of disc degeneration at C5-C6 using published methods [37,38]. The specimens were then carefully dissected to remove the paraspinal muscles while preserving all of the spinal ligaments and to fully expose, but keep intact, the left C5-C6 facet joint capsule. The C2 and T1 vertebrae were cleaned and cast in aluminum cups via crossed Kirschner-wires inserted through the vertebral bodies and additional wires inserted in the spinous processes that coupled to the casting material (Flow Stone; Whip Mix Corp.; Louisville, KY). A customized potting frame was used to ensure that the specimen's anteroposterior and coronal alignments were cast maintaining the natural neutral lordotic position of each specimen for testing. Briefly, this frame supports the specimen during casting of both ends, ensures the casting cups remain parallel to enable proper coupling to the loading frame after potting, and allows freedom in positioning the cups to maintain the natural lordosis of each specimen.

A customized testing frame was used to impose controlled flexion and extension and to enable simultaneous measurement of the relative vertebral motions and the C5-C6 facet joint contact pressure during testing (Fig. 1). The base of the specimen was rigidly

Table 1 Summary of disc degeneration, probe orientation, and the neutral position ROM and pressure for each specimen.

Specimen	Age	C5-C6 Disc degeneration[a]	Probe off-perpendicular angle in sagittal plane (deg)	Isolated tests ROM (deg)		Neutral position ROM (deg)		Neutral position pressure changes (kPa)	
				Global (C2-T1)	Segmental (C5-C6)	Global (C2-T1)	Segmental (C5-C6)	Min	Max
#1	37	none	3.5	85.4	18.8	73.4	15.7	−6.4	36.9
#2	51	none	1.5	51.2	10.2	34.1	6.8	−30.0	−2.5
#3	65	none	5.4	48.0	8.6	33.3	5.6	−9.3	13.2
#4	54	none	2.8	57.3	6.3	38.2	4.7	−18.4	0.6
#5	78	moderate	0.3	32.5	5.3	20.5	2.9	−8.8	2.5
#6	69	minimal	0.7	50.9	11.3	33.1	7.2	−13.7	11.6
Mean	**59**	**-**	**2.4**	**54.2**	**10.1**	**38.7**	**7.1**	**−14.4**	**10.4**
St. Dev.	15	-	1.9	17.4	4.8	18.0	4.5	8.7	14.4

Note: St. Dev. = Standard deviation.
[a]based on published rating scales [37,38].

fixed to the test frame through the T1 casting cup that was coupled to a six-axis load cell (model 4386, RA Denton Inc.; Rochester Hills, MI). Sagittal bending moments were applied using a cable and pulley system connected to a bar attached to the C2 cup (Fig. 1(*b*)). A customized LabVIEW program regulated the piston pressure applied to the cabling system exerting a force of approximately 5 N. The force developed over one second and was held for one second. The cable was attached 401 mm and 346 mm from the center of the C2 cup so that physiologic moments of at least 2 Nm [13,39,40] were applied in flexion and extension, respectively. Because specimens exhibit different flexibility in flexion than in extension and there is a difference in the cable's attachment for each bending direction, applied moments were greater in flexion than in extension. Mechanical guides constrained the moment application bar to ensure that only sagittal moment was applied to the top of the specimen. The test frame was integrated with an optical-analog tracking system (PEAK, Vicon; Denver, CO) that tracked the three-dimensional motions of the specimen during loading and was synchronized to also acquire data from the load cell and a pressure transducer (probe) inserted in the left C5-C6 facet joint, at a rate of 600 Hz. The combined weight of the top cup, potting material, and moment application bar comprised a preload of 14 N. Greater preloads were not imposed because their application rendered the osteoligamentous specimens unstable causing them to bend out of the sagittal plane even in the resting position.

During sagittal bending, both visual markers and a pressure probe were used to acquire kinematic and joint pressure data. At each vertebral level ranging from C4 to C7, three spherical silver reflective polystyrene beads (6.35 mm diameter) were affixed to each of the right and left lateral tubercles and at the mid-height along the mid-sagittal plane of the anterior surface of the vertebral body (Fig. 1(*b*)). Two reflective beads were also affixed to each of the C2 and T1 casting cups to track the global motions of the entire cervical spine specimen. Four infra-red cameras, with resolution of 0.6° for rotations and 0.2 mm for translation, simultaneously tracked the motion of the reflective markers during testing, at 120 Hz. A tip-mounted pressure probe was used to measure the contact pressure in the left C5-C6 facet joint, using an approach that maintains the integrity of the joint and does not require transection of the joint capsule for its insertion [18]. For this approach, a hole was drilled under fluoroscopic guidance in the inferior aspect of the C5 lateral mass with an orientation directed perpendicular to the C6 articular surface in the sagittal plane (Fig. 1). Care was taken to avoid the extreme inferior portion of the C5 lateral mass that does not articulate with the C6 surface. A cylindrical pressure probe (XCEL-100-50A; Kulite Semiconductor Products; Leonia, NJ) with a circular piece of rubber (0.5 mm-thick, 2 mm-diameter) fit at its tip was press-fit in the bone (Fig. 1). The probe has a deformable membrane featuring miniature leadless strain sensors which is located in a recess at the extremity of the probe and is 97% accurate for pressures in the range detected for this study. The probe was inserted such that the rubber piece was in contact with the C6 articular surface on one side and with the sensing membrane of the sensor on the other side. The angle of the probe relative to the C6 articular surface for each specimen was measured in the sagittal plane as the angle between the axis of the probe and the facet surface using the fluoroscopic images and the OsiriX software (Pixmeo Sarl, Geneva, Switzerland) to verify that the probe was perpendicular to the C6 articular surface (Table 1).

After probe insertion, the specimen was manually exercised for five times through its full range of motion to verify that the probe signal output was responsive to the contact established by the opposing C6 articular surface. This also served as specimen preconditioning. Because maximal facet contact occurs when the spine is farthest from its neutral posture [6,36], isolated flexion and extension moments were then applied with the specimen initially resting in a flexed or extended position away from its neutral position. After acquiring kinematic, kinetic and pressure data in isolated flexion and extension, each specimen was manually exercised through its entire range of motion starting with the specimen in its natural most-flexed position and undergoing further flexion, reversal towards full extension, and then being returned to its initial flexed position. During this sagittal bending test, the moment-angle relationship was defined in order to provide context for the joint pressure responses defined in the isolated bending tests.

For each of the isolated flexion and extension tests, the forces, moments, motions, and pressures in the C5-C6 facet joint were continuously measured prior to, during, and after the application of moment (Fig. 2). The images from the infra-red cameras were analyzed with PEAK software (Motus Version 8.0) for three-dimensional reconstruction and calculation of the global (C2–T1) and segmental (C5-C6) sagittal angular rotations during bending (Fig. 2(*a*)). The change in sagittal moment (ΔM) and the rate of loading ($\Delta M/t$) were calculated using the maximum moment and the moment measured at the onset of the application of moment, i.e., during the loading phase (Fig. 2(*b*)). Similarly, the change in global angle ($\Delta\theta_g$), the change in segmental C5-C6 angle ($\Delta\theta_s$), and the change in pressure (ΔP) during the moment loading phase were also calculated using the respective datasets. Linear regression was used to evaluate the relationship between the change in applied moment and the global angle ($\Delta\theta_g/\Delta M$), as well as the change in pressure ($\Delta P/\Delta M$). The relationship between the change in segmental angle and pressure ($\Delta P/\Delta\theta_s$) was also determined by calculating the slope of the best-fit line of the segmental angle-pressure data. Regressions were performed for the pressure, moment, and angle responses during the moment loading phase (Fig. 2(*b*)). A customized Matlab code (MathWorks, Natick, MA) was used to quantify the tangent slope of each response over its linear region; briefly, a best-fit line was fit over the region starting with the onset of moment application through the response over

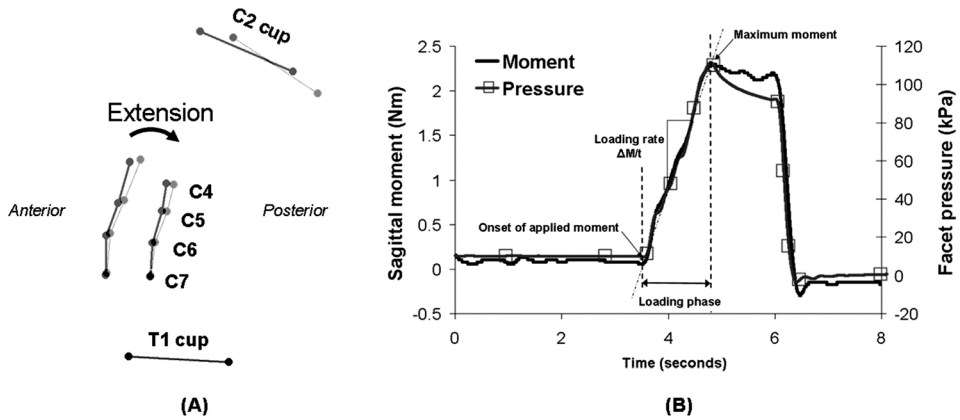

Fig. 2 (*a*) **Reconstruction in PEAK software of the tracking markers of a representative specimen (Specimen #1) in its initial position (bold segments) and under applied extension (light segments). The markers for each segment, as well as the C2 and T1 potting cups, are also labeled. (*b*) Time history trace of the corresponding applied extension moment and the associated pressure changes developed in the facet joint during loading. The rate of loading is defined by the ΔM/t slope of the moment trace during the loading phase between the onset and maximum moments.**

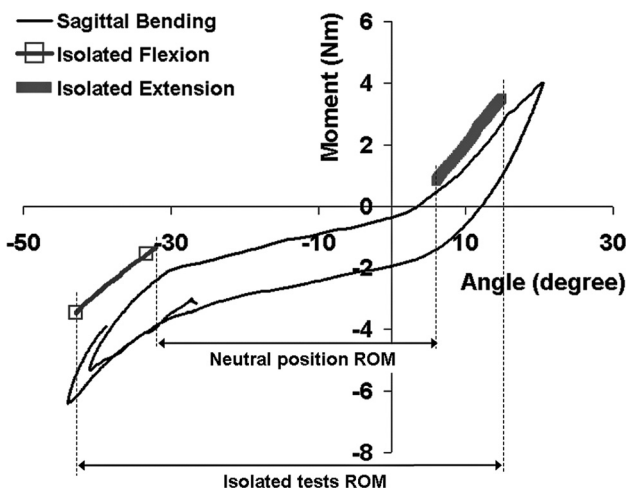

Fig. 3 Example of moment-angle curves measured during the sagittal bending test and the isolated flexion and extension tests for Specimen #4. The ROMs of the neutral position and of the isolated tests are also shown.

the region in which the associated coefficient of determination (R^2) of the fit line was 0.95 or greater. All outcomes were averaged across the specimens and paired t tests were used to compare the relationships determined for flexion to those for extension. For each specimen, the relationship between the global angle and bending moment developed during the sagittal bending test was defined to complement and verify that the angle-moment response of the specimens to the isolated bending tests corresponded to their elastic zone response (Fig. 3). The range of motion (ROM) was measured for the combined isolated flexion and extension tests (isolated tests ROM) and over the angular span between the onset of these tests (neutral position ROM) for each specimen (Fig. 3). Facet contact pressures were also measured during the sagittal bending tests for a range of angles corresponding to the neutral position ROM from the isolated tests (Table 1).

3 Results

In general, the pressure probe was inserted perpendicular to the facet surface for the specimens in this study, with an average angle of $2.4 \pm 1.9°$ off of the perpendicular to the articular surface (Fig. 1(*a*), Table 1). Based on the imaging, the probe was generally placed in the most inferior region of the C5 lateral mass that still made contact with the underlying C6 articular surface when the spine was in its resting position. The resolution of the pressure probe was 0.4 ± 0.1 kPa and the error in making pressure measurements was 1.0 ± 1.2 kPa for these studies. Similarly, the resolution and error associated with the angle measurements of the motion tracking system were $0.40 \pm 0.05°$ and $0.40 \pm 0.30°$, respectively.

The changes in anteroposterior (ΔFx) and transverse (ΔFy) forces during application of the sagittal bending moment were small (under 1.7 N) and the associated change in axial force (ΔFz) remained below 7 N (Table 2). The changes in out-of-plane moments (ΔMx, ΔMz) were less than 0.12 Nm and small compared to the mean applied sagittal moments (ΔMy) that were 2.7 ± 0.3 Nm in flexion and 2.4 ± 0.3 Nm in extension (Table 2). The cervical specimens rotated by $9.4 \pm 2.3°$ in flexion and by $9.6 \pm 0.8°$ in extension for the isolated flexion and extension moments (Table 3); the corresponding segmental rotation at C5-C6 was $1.2 \pm 0.3°$ in flexion and $1.6 \pm 0.7°$ in extension. The mean neutral position range of motion that all specimens exhibited between the isolated flexion and extension tests was $38.7 \pm 18.0°$ globally and $7.1 \pm 4.5°$ at C5-C6; the mean global and segmental ranges of motion for the combined isolated tests were $54.2 \pm 17.4°$ and $10.1 \pm 4.8°$, respectively (Fig. 3; Table 1). The ranges of motion were very similar between specimens with little variation from the mean for the majority of the specimens (Fig. 3; Table 1).

Although the magnitude of applied sagittal moments was significantly different ($p = 0.021$) for flexion and extension, the rate of loading and the changes in global and segmental angles were not significantly different between flexion and extension (Table 3). In addition, for the isolated moment loading the relationships between the change in applied moment and the change in global angle were linear and exhibited consistent magnitudes among specimens in each of flexion and extension (Table 3, Fig. 4). The mean flexibility ($\Delta\theta_g/\Delta M$) for the applied moment was 3.8 ± 0.8 deg/Nm in flexion and was not significantly different from that in extension (4.0 ± 0.7 deg/Nm) (Table 3). The global angle-moment relationships were linear in both flexion and extension (Fig. 4); the R^2 values of the fits (0.98 ± 0.02) were not different between the directions of applied moment. The relationships were offset from the origin since the specimens were in their natural most-flexed and most-extended positions at the onset of the flexion and extension tests, respectively (Figs. 3 and 4). However, the

Table 2 Summary of the changes in the forces and moments as measured by the 6 DOF load cell for sagittal bending for each specimen.

	ΔFx (N)		ΔFy (N)		ΔFz (N)		ΔMx (Nm)		ΔMy (Nm)		ΔMz (Nm)	
Specimen	Ext	Flex	Ext	Flex	Ext	Flex	Ext	Flex	Ext	Flex	Ext	Flex
#1	1.1	−8.0	0.0	−1.4	−4.3	−7.1	0.1	−0.6	2.2	−2.7	0.0	−0.1
#2	0.9	−0.6	0.6	1.7	−4.3	−7.1	0.1	1.2	2.3	−2.7	−0.1	−0.2
#3	0.9	−0.6	−0.3	0.6	−1.4	−5.7	0.0	0.8	1.9	−2.4	0.0	0.0
#4	1.1	−1.4	0.0	0.9	−2.9	−5.7	0.1	0.5	2.7	−2.6	−0.1	0.0
#5	1.7	−0.3	0.0	0.3	−2.9	−5.7	0.2	0.2	2.7	−3.2	0.0	−0.1
#6	1.4	0.9	0.0	1.7	−1.4	−7.1	0.0	0.5	2.3	−3.0	−0.1	0.3
Mean	**1.2**	**−1.7**	**0.0**	**0.6**	**−2.9**	**−6.4**	**0.1**	**0.4**	**2.4**	**−2.7**	**0.0**	**0.0**
St. Dev.	0.3	3.2	0.3	1.2	1.3	−1.8	0.1	0.6	0.3	0.3	0.1	0.2

Note: St. Dev. = Standard deviation.

Table 3 Summary of relevant pressure, kinematics, and mechanics in the sagittal plane for the isolated applied bending moments.

	ΔMy (Nm)		$\Delta\theta_g$ (deg)		$\Delta\theta_s$ (deg)		ΔP (kPa)		ΔMy/t (Nm/sec)		$\Delta\theta_g/\Delta$My (deg/Nm		ΔP/ΔMy (kPa/Nm)		$\Delta P/\Delta\theta_s$ (kPa/deg)	
Specimen	Ext	Flex	Ext	Flex	Ext	Flex	Ext	Flex	Ext	Flex	Ext	Flex	Ext	Flex	Ext	Flex
#1	2.2	−2.7	10.9	−5.9	1.9	−1.0	102	−17	1.8	−2.7	4.2	4.4	47	49	48	36
#2	2.3	−2.7	9.6	−9.0	1.7	−1.6	39	1	2.9	−2.3	3.9	3.3	16	−1	23	−1
#3	1.9	−2.4	8.6	−9.6	1.4	−1.4	90	−11	1.6	−1.8	5.0	4.1	130	7	148	8
#4	2.7	−2.6	8.9	−12.4	0.5	−0.8	69	−26	2.9	−2.1	3.3	4.9	43	19	−182	62
#5	2.7	−3.2	9.5	−8.3	1.6	−0.9	33	−6	2.2	−2.5	3.4	2.7	12	2	16	9
#6	2.3	−3.0	10.2	−11.0	2.7	−1.4	72	−2	1.6	−5.1	4.4	3.6	60	1	56	1
Mean	**2.4**	**−2.7**	**9.6**	**−9.4**	**1.6**	**−1.2**	**67**	**−10**	**2.2**	**−2.8**	**4.0**	**3.8**	**51**	**13**	**18**	**19**
St. Dev.	0.3	0.3	0.8	2.3	0.7	0.3	27	10	0.6	1.2	0.7	0.8	43	19	109	25
P-value	0.021[a]		0.860		0.130		0.002[a]		0.404		0.635		0.099		0.978	

Note: St. Dev. = Standard deviation.
[a]significant difference (p-value < 0.05) between flexion and extension.

specimens displayed greater flexibility in flexion than in extension, as evidenced by the greater rotation in flexion than in extension (Fig. 4). One specimen was initially flexed by 65°, but the remaining specimens were initially flexed at an angle of 10–30° (Fig. 4(*a*)). In extension, the initial offset was only 10° for four of the specimens, and varied by only five degrees for the other two (Fig. 4(*b*)).

Not surprisingly, the facet joint contact pressure exhibited different responses in flexion and in extension. In the region around the neutral position for each specimen, facet pressure ranged from −14.5–10.3 kPa (Table 1). Flexion resulted in a decrease in the contact pressure in the C5-C6 facet joint, whereas joint pressure increased during extension (Table 3, Fig. 5). The average change in pressure (−10.3 ± 9.7 kPa) in flexion was significantly smaller ($p = 0.002$) than the 67.6 ± 26.9 kPa pressure change in extension (Table 3). In general, the relationship between joint contact pressure and the applied extension moment was linear over the loading phase for most of the specimens with an average ΔP/ΔM of 51.4 ± 42.6 kPa/Nm (Table 3, Fig. 5). However, the region of linearity varied between specimens and was not sustained over the entire loading phase for all specimens (Fig. 5). For half of the specimens, the C5-C6 facet pressure increased linearly with the applied extension moment until the maximal moment was reached, with ΔP/ΔM ranging from 12.4–46.9 kPa/Nm (Table 3, Fig. 5). For the other three specimens, the pressure changed more dramatically as the extension moment was increased, but then leveled off before the maximum moment was reached (Fig. 5). In flexion, the pressure changes were very small and 3–37 times smaller than those detected in extension (Table 3). Consequently, the average ΔP/ΔM for flexion (13.0 ± 19.0 kPa/Nm) was smaller than that in extension, despite not being significantly different. The relationship between facet contact pressure and the change in segmental angle was also generally linear with an average $\Delta P/\Delta\theta_s$ slope of 19.3 ± 24.7 kPa/deg in flexion and 18.0 ± 108.9 kPa/deg in extension, respectively (Table 3). Because of their variability, these values were not significantly different between flexion and extension.

4 Discussion

This study is the first to describe how pressure develops in the facet joint of a cadaveric cervical spine during physiologic sagittal bending. Moments greater than 2 Nm were applied but since the specimens had different bending stiffnesses, the magnitude of the average flexion and extension moments were 2.7 Nm and 2.4 Nm, respectively (Table 2). Contact pressure in the inferior region of the facet joint increased during extension as the articular surfaces came in contact, and decreased slightly during flexion as the joint opened (Table 3). The mean increase in pressure of 67.6 ± 26.9 kPa that was generated by the 2.4 Nm change in moment during extension is relatively small in comparison to other studies of this joint. For example, in a study using pressure-sensitive paper in the lumbar cadaveric spine, pressure increased by over 1.4 MPa during a 6° extension [41]. Further, a finite element model of an isolated human cervical facet joint predicted contact pressures that were 1–2 orders of magnitude greater (0.2–5.3 MPa) than the pressures reported here, for 18° of extension [24]. In addition, both el-Bohy et al. [36] and Wiseman et al. [28] have reported much higher pressures (0.25–3.7 MPa) to be developed in the lumbar facet under more extreme loading conditions, such as a combined 700 N compression coupled with a 15 Nm extension moment. Therefore, examining the pressure data from the current study in the context of existing studies, it is difficult to make meaningful direct comparisons between contact pressures in the

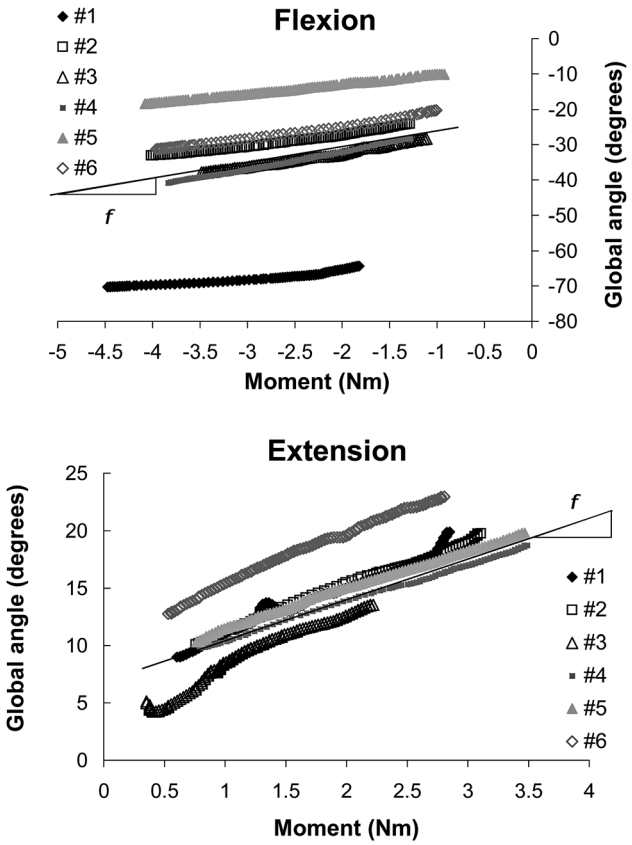

Fig. 4 Global angle-moment responses from the applied isolated flexion and extension tests showing linear relationships for both loading scenarios and all specimens. The linear relationship was defined by the flexibility slopes ($\Delta\theta_g/\Delta My$) labeled f on the graphs.

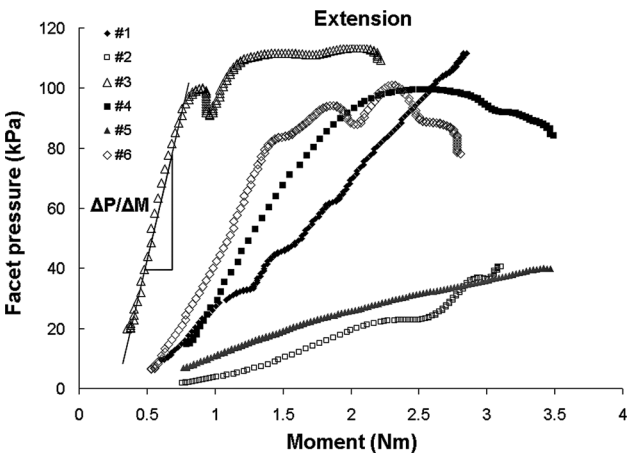

Fig. 5 Pressure-moment responses from the isolated extension tests, showing generally linear relationships for all specimens as defined by the ΔP/ΔM slopes labeled on the graph

facet across different regions of the spine. Certainly, the compressive load in the lumbar spine is greater than that in the cervical spine and the compressive loads used in those lumbar spine studies were substantially larger than the compressive preload used in the current study. This preload (14 N) was less than that used in previous studies (36–66 N) that were aimed at mimicking the weight of the head [42–45]; as such, the cervical facet pressures here may be slight underestimates of the true pressures established in the joint. However, the effect of a higher preload may be mitigated as the discs of at least four out of six specimens were not degenerated and would have borne a large part of any additional preload. Furthermore, a larger axial preload would have exaggerated any motion and/or deformation of the flexible osteoligamentous specimens and cause them to bend in both the sagittal and lateral planes. However, implementation of a follower preload could have provided additional stability [46,47].

The applied sagittal bending moment experienced by the specimen was not a pure sagittal moment based on the test configuration. This was confirmed by the slight changes in forces and out-of-plane moments (Table 2). Although the change in compressive force (ΔFz) was the largest of all loads, it nevertheless remained quite small in both flexion and extension (Table 2). Similarly, the out-of-plane moments that developed were less than 4% of the applied sagittal moment, except for the lateral bending moment (ΔMx) in flexion which reached approximately 15% of the sagittal moment (Table 2). Given all of these data, the coupled loads and moments were negligible and likely did not influence the pressure measurements. Therefore, the actual loading of the specimen may be considered as a physiologic combined compressive-bending loading.

The facet contact pressure detected in the joint when it was close to its natural neutral position was very small (Table 1). This is not surprising, given that the intervertebral rotations occurred under small moments, which implies that the articular surfaces may be sliding relative to each other without significantly modifying the contact with the probe tip. The small segmental rotations measured under small moments in the region around the neutral posture ($7.1 \pm 4.5°$) (Table 1) are consistent with other reports for the cervical and lumbar spines [48–51]. The magnitude of the facet pressure close to the neutral position may be increased if the posterior musculature had been replicated in the test setup; this effect was not tested. However, pilot studies did reveal that only very small pressure changes were developed in the facet when the spine was around its neutral position (Fig. 3). Therefore specimens were specifically tested in isolated flexion and extension starting in their natural most-flexed and most-extended positions, respectively, in order to induce measureable pressure changes in the C5-C6 facet joint (Figs. 2 and 5). In order to ensure that the pressure responses from those isolated tests were interpreted appropriately in the context of each specimen's neutral position, the moment-angle responses from the isolated bending tests were individually superimposed on those generated during the sagittal bending test (Fig. 3). This superimposition confirmed that the moment-angle responses from the isolated flexion and extension tests were aligned with the flexion and extension elastic zones of the moment-angle response from the sagittal bending test [48]. In fact, the moment-angle responses of the sagittal bending tests (Fig. 3) are consistent with previous reports of cadaveric responses [52]. Similarly the measured average global and segmental ROMs from the combined isolated tests (Table 1) are also both similar to the 41–94.3° global and 9.7–23° segmental ranges of motion reported in the literature [53]. In this context, the application of isolated unidirectional flexion and extension moments generated rotations in the cervical specimens that were consistent with normal spinal responses and; consequently, so too can the associated vertebral rotations and contact pressures in the facet joint be taken as representative of physiological responses.

Pressure changes in the facet joint during physiologic extension varied across specimens despite consistent placement of the pressure probe in the inferior region of the C5-C6 joint (Table 3, Fig. 1(*a*)). This was in agreement with the reported variations in maximum pressures in the facet joints of lumbar motion segments extended by up to 6° [41]. Although, the spatial distribution of pressure in both cervical and lumbar facet joints is not uniform over the articular surfaces during extension, studies using pressure-sensitive paper introduced in the joint or computational models have reported that articular contact generally develops in the inferior region of the articular surface but near its edge, during extension [24,28,41,50]. With this in mind, fluoroscopic imaging

was used to ensure careful positioning of the probe in the inferior region of the facet in all specimens and with an orientation as close to perpendicular to the surface as possible. Both of these factors were confirmed to be similar among specimens in this study (Table 1). The probe was inserted in the inferior region of the joint and positioned at the location where contact pressure was the most likely to develop in extension in all the specimens. In addition, previous studies with this pressure measurement technique demonstrated that a probe orientation with only a small off-perpendicular angle (less than 5°) does not significantly affect the pressure measurements [18]. As such, the 2.4 ± 1.9 off-perpendicular angle measured in this study (Table 1) suggests that any variability in the pressure measurements detected here may likely be attributed to variability in the specimens themselves, either anatomic or degenerative qualities. Although the specimens were screened for gross defects, such as osteophytes and facet/disc space narrowing, subtler cartilaginous degeneration could not be controlled for and thus may have affected the contact medium for the sensing element at the tip of the pressure probe. Similarly, meniscoids sliding underneath the probe tip during motion may also affect pressure measurements, which may explain why half of the specimens displayed a partial linear pressure-moment response while the response was fully linear in the other half of the specimens (Fig. 5). During loading, the opposing cartilaginous surfaces, the meniscoids, and the capsular ligaments forming the facet joints all undergo different relative motions depending on the initial joint orientation and the magnitude and direction of loading. Given that these individual structural elements of the facet vary from specimen to specimen and across spinal levels, it is not surprising that the contact pressure responses exhibit different behaviors across specimens (Fig. 5).

In the current study, the pressure changes in flexion were negative and even smaller than those in extension (Table 3), which is in contrast to pressure responses from previous studies. Kumaresan et al. [24] reported positive contact pressure to develop at the anterior edge of the articular surface of the cervical facet joint under flexion. Similarly, a computational model of a lumbar motion segment with an arthroplastic disc device also reported increased contact pressure in the anterior region of the facet when subjected to flexion moments between 3 and 7.5 Nm [16]. This discrepancy in pressures during flexion for our experimental study and the models is likely due to the fact that the pressure probe was located in the inferior region of the facet joint (Fig. 1), which optimized pressure measurements in extension. The inferior region of the joint has been previously reported to be the region where contact between the articular surfaces occurs during extension and where maximum pressures have been measured in cadaveric lumbar motion segments [28,36,41,48]. In a study by el-Bohy et al. [36], a pressure of 0.2 MPa was measured using a similar approach with a tip-mounted pressure transducer in the lumbar joint under 600 N of compression and 15 Nm of extension. Even higher pressures were reported in studies by Dunlop et al. [41] and Wiseman et al. [28] using pressure-sensitive paper placed in the joint. In those studies, contact pressure was also reported to occur in the inferior.region [28,41]. Finally, facet strains and forces have been used also to estimate pressure at specific regions of the articular surface for combined compression-moment loading in the lumbar spine; in that work 2 MPa of pressure was reported to develop at the inferior tip of the articular surface [50]. Despite the more-horizontal orientation and greater mobility of the cervical facets than those in the lumbar spine, facet contact was expected also to occur in the inferior region during extension owing to the fact that facets throughout the spine play the role of limiting vertebral rotation.

The inferior region of the joint opened during flexion and moved the sensing membrane of the probe away from the cartilage which may have led to the generation of the negative pressure change. In fact, the response in flexion is also sensitive to the specific loading paradigm and may have been greater had an axial preload higher than 14 N been applied. A higher axial preload would add additional flexion moment and that could lead to greater joint opening during flexion. However, facet joint separation was not measured directly in this study and is only inferred from the kinematics measurements. Additional work is needed to integrate the facet motions and loading with tissue responses in the cervical and lumbar region. The small average magnitude of pressure change may likely be due to the weak and easy-to-break contact between the probe tip and the cartilage. Therefore, it is likely that the negative pressure changes observed here in flexion reflect the relief of the necessary minimal contact pressure that was initially applied prior to testing in order to confirm that the probe was correctly positioned. However, the variability in this measurement between specimens which was as large as the average pressure change (Table 3) likely reflects a difference in the degree of contact between the probe tip and the cartilage from specimen to specimen. The largest negative pressure changes could have resulted from a vacuum effect at the tip of the probe. Since the probe was press-fit into the joint space in close contact with the superior cartilage surface of the C6 articular pillar, there was no air between the sensor tip and underlying cartilage. In fact, all but one specimen exhibited absolute negative pressures during flexion (below the referenced atmospheric pressure), which suggests that the separation of the contact surfaces may have induced a local vacuum effect. Regardless, these results suggest that at least the inferior aspect of the joint undergoes an element of distraction during physiologic flexion, which is consistent with other reports that the facet joint capsule undergoes tension in the inferior (dorsal) region during flexion [2,54,55].

It is not clear whether facet pressure changes developed during extension are caused by the moment application or the specimen's rotation (Table 3). Actually, facet pressure has been reported to increase with extension angle [24,29,41] and facet force has been reported to increase with the extension moment [50]. This study is the first to establish a relationship between facet pressure and both the changes in moment and segmental angle for sagittal bending in the cervical spine (Table 3). To a certain degree, these relationships are not surprising since when the spine extends it rotates and brings the articular surfaces of the facet joint together, in the process resisting that moment. Accordingly, a general linear relationship with R^2 values ranging from 0.63–0.99 (data not shown), was also observed between the moment and the sagittal angle in extension (Fig. 4). This moment-angle relationship is consistent with published reports [56]; it also demonstrates that both moment and rotation increase simultaneously during sagittal bending. Therefore, under physiologic loading conditions it is likely that the change in pressure in the facet joint may be attributed to *both* the change in moment and the change in segmental angle that is established. However, as kinematic studies have reported altered shear and distraction for otherwise similar angular rotations of a cervical motion segment in whiplash simulations [6], future studies may identify differing pressure-moment-rotation relationships in nonphysiologic loading conditions. Measuring facet contact force could also provide important insight into the local facet mechanics during loading in various configurations. The technique employed in this study did not permit direct quantification of the contact area to calculate facet forces. However, recent studies have begun to investigate this using imaging approaches coupled with biomechanics [57].

The mechanical behavior of the facet joint is susceptible to any change in its local mechanics. Biomechanical investigations have led to the accepted hypothesis that disc degeneration precedes facet osteoarthritis [58,59]. Surgical interventions aimed at replacing a failing intervertebral disc cannot completely restore all of the functions of the disc and; therefore, affect the behavior of the associated facet joints. Although motion preservation devices have been designed to reduce adjacent segment disease, several clinical investigations have reported a significant incidence of facet disease at the implanted level [60–62]. The mechanisms leading to facet arthritis are not well understood but they are likely linked to a change in the contact pressure imposed

to the cartilage matrix during altered motion. Even a slight change in the mechanical behavior of the joint could modify either or both the pressure magnitude and distribution in this joint significantly. Nonetheless, the contact pressures developed in an intact facet joint that were defined in this study for normal ranges of loading and motion in the neck can provide a foundation for comparison for other more-complicated potential exposures for this joint, such as trauma or a surgical intervention such as fusion, disc replacement, or laminectomy. Although this pressure measurement technique has obvious positional limitations, it is minimally-invasive to the joint as a whole and adequate for facet pressure measurements in intact, instrumented, or surgically modified cadaveric spines and may serve as a template for other loading paradigms.

Acknowledgment

This project was supported by research funding from Synthes, Inc. and the Catharine Sharpe Foundation and a Research Fellowship from the Neurosurgery Research & Education Foundation.

References

[1] Panjabi, M. M., Simpson, A. K., Ivancic, P. C., Pearson, A. M., Tominaga, Y., and Yue, J. J., 2007, "Cervical Facet Joint Kinematics During Bilateral Facet Dislocation," Eur. Spine J., **16**, pp. 1680–1688.
[2] Winkelstein, B. A., Nightingale, R. W., Richardson, W. J., and Myers, B. S., 2000, "The Cervical Facet Capsule and its Role in Whiplash Injury: A Biomechanical Investigation," Spine, **25**, pp. 1238–1246.
[3] Shanmuganathan, K., Mirvis, S. E., and Levine, A.M., 1994, "Rotational Injury of Cervical Facets: CT Analysis of Fracture Patterns With Implications for Management and Neurologic Outcome," Am. J. Roentgenol., **163**, pp. 1165–1169.
[4] Dvorak, M. F., Fisher, C. G., Fehlings, M. G., Rampersaud, Y. R., Oner, F. C., Aarabi, B., and Vaccaro, A. R., 2007, "The Surgical Approach to Subaxial Cervical Spine Injuries: An Evidence-Based Algorithm Based on the SLIC Classification System," Spine, **32**, pp. 2620–2629.
[5] Pearson, A. M., Ivancic, P. C., Ito, S., and Panjabi, M. M., 2004, "Facet Joint Kinematics and Injury Mechanisms During Simulated Whiplash," Spine, **29**, pp. 390–397.
[6] Stemper, B. D., Yoganandan, N., Gennarelli, T. A., and Pintar, F. A., 2005, "Localized Cervical Facet Joint Kinematics Under Physiological and Whiplash Loading," J. Neurosurg. Spine, **3**, pp. 471–476.
[7] Ivancic, P. C., Ito, S., Tominaga, Y., Rubin, W., Coe, M. P., Ndu, A. B., Carlson, E. J., and Panjabi, M. M., 2008, "Whiplash Causes Increased Laxity of Cervical Capsular Ligament," Clin. Biomech. **23**, pp. 159–165.
[8] Raynor, R. B., Pugh, J., and Shapiro, I., 1985, "Cervical Facetectomy and its Effect on Spine Strength," J. Neurosurg., **63**, pp. 278–82.
[9] Zdeblick, T. A., Abitbol, J. J., Kunz, D. N., McCabe, R. P., and Garfin, S., 1993, "Cervical Stability After Sequential Capsule Resection," Spine, **18**, pp. 2005–2008.
[10] Bogduk, N., and Marsland, A., 1988, "The Cervical Zygapophysial Joints as a Source of Neck Pain," Spine, **13**, pp. 610–617.
[11] Dreyer, S. J., and Dreyfuss, P. H., 1996, "Low Back Pain and the Zygapophysial (Facet) Joints," Arch. Phys. Med. Rehabil., **77**, pp. 290–300.
[12] Cavanaugh, J. M., Lu, Y., Chen, C., and Kallakuri, S., 2006, "Pain Generation in Lumbar and Cervical Facet Joints," J. Bone Joint Surg. Am., **88**(2), pp. 63–67.
[13] Chang, U. K., Kim, D. H., Lee, M. C., Willenberg, R., Kim, S. H., and Lim, J., 2007, "Changes in Adjacent-Level DiscPressure and Facet Joint Force After Cervical Arthroplasty Compared With Cervical Discectomy and Fusion," J. Neurosurg. Spine, **7**, pp. 33–39.
[14] Rousseau, M. A., Bradford, D. S., Bertagnoli, R., Hu, S. S., and Lotz, J. C., 2006, "Disc Arthroplasty Design Influences Intervertebral Kinematics and Facet Forces," Spine J., **6**, pp. 258–266.
[15] Rundell, S. A., Auerbach, J. D., Balderston, R. A., and Kurtz, S. M., 2008, "Total Disc Replacement Positioning Affects Facet Contact Forces and Vertebral Body Strains," Spine, **33**, pp. 2510–2417.
[16] Schmidt, H., Midderhoff, S., Adkins, K., and Wilke, H. J., 2009, "The Effect of Different Design Concepts in Lumbar Total Disc Arthroplasty on the Range of Motion, Facet Joint Forces and Instantaneous Center of Rotation of a L4-5 Segment," Eur. Spine J., **18**, pp. 1695–1705.
[17] Luan, F., Yang, K. H., Deng, B., Begeman, P. C., Tashman, S., and King, A. I., 2000, "Qualitative Analysis of Neck Kinematics During Low-Speed Rear-End Impact," Clin. Biomech., **15**, pp. 649–657.
[18] Jaumard, N. V., Bauman, J. A., Welch, W. C., and Winkelstein, B. A., 2011, "Pressure Measurement in the Cervical Spinal Facet Joint: Considerations for Maintaining Joint Anatomy and an Intact Capsule," Spine, **36**, pp. 1197–1203.
[19] Siegmund, G. P., Davis, M. B., Quinn, K. P., Hines, E., Myers, B. S., Ejima, S., Ono, K., Kamiji, K., Yasuki, T., and Winkelstein, B. A., 2008, "Head-Turned Postures Increase the Risk of Cervical Facet Capsule Injury During Whiplash," Spine, **33**, pp. 1643–1649.
[20] Pal, G. P., and Sherk, H. H., 1988, "The Vertical Stability of the Cervical Spine," Spine, **13**, pp. 447–449.
[21] Pal, G. P., and Routal, R. V., 1986, "A Study of Weight Transmission Through the Cervical and Upper Thoracic Regions of the Vertebral Column in Man," J. Anat., **148**, pp. 245–261.
[22] Buttermann, G. R., Kahmann, R. D., Lewis, J. L., and Bradford, D. S., 1991, "An Experimental Method for Measuring Force on the Spinal Facet Joint: Description and Application of the Method," J. Biomech. Eng., **113**, pp. 375–386.
[23] Sawa, A. G., and Crawford, N. R., 2008, "The Use of Surface Strain Data and a Neural Networks Solution Method to Determine Lumbar Facet Joint Loads During in Vitro Spine Testing," J. Biomech., **41**, pp. 2647–2653.
[24] Kumaresan, S., Yoganandan, N., and Pintar, F. A., 1998, "Finite Element Modeling Approaches of Human Cervical Spine Facet Joint Capsule," J. Biomech., **31**, pp. 371–376.
[25] Kang, H., Park, P., La Marca, F., Hollister, S. J., and Lin, C. Y., 2010, "Analysis of Load Sharing on Uncovertebral and Facet Joints at the C5-6 Level with Implantation of the Bryan, Prestige LP, or ProDisc-C Cervical Disc Prosthesis: An in Vivo Image-Based Finite Element Study," Neurosurg. Focus, **28**(6), pp. E9.
[26] Panzer, M. B., and Cronin, D. S., 2009, "C4-C5 Segment Finite Element Model Development, Validation, and Load-Sharing Investigation," J. Biomech., **42**, pp. 480–490.
[27] Liu, F., Cheng, J. S., Komistek, R. D., and Mahfouz, M. R., 2008, "Normal, Fused, and Degenerative Cervical Spines: A Comparative Study of Three-Dimensional in Vivo Kinetics," J. Bone Joint Surg. Am., **90**(4), pp. 85–89.
[28] Wiseman, C. M., Lindsey, D. P., Fredrick, A. D., and Yerby, S. A., 2005, "The Effect of an Interspinous Process Implant on Facet Loading During Extension," Spine, **30**, pp. 903–907.
[29] Niosi, C. A., Wilson, D. C., Zhu, Q., Keynan, O., Wilson, D. R., and Oxland, T. R., 2008, "The Effect of Dynamic Posterior Stabilization on Facet Joint Contact Forces: an in Vitro Investigation," Spine, **33**, pp. 19–26.
[30] Wilson, D. C., Niosi, C. A., Zhu, Q. A., Oxland, T. R., and Wilson, D. R., 2006, "Accuracy and Repeatability of a New Method for Measuring Facet Loads in the Lumbar Spine," J. Biomech., **39**, pp. 348–353.
[31] Oxland, T. R., Panjabi, M. M., Southern, E. P., and Duranceau, J. S., 1991, "An Anatomic Basis for Spinal Instability: A Porcine Trauma Model," J. Orthop. Res., **9**, pp. 452–462.
[32] Liau, J. J., Hu, C. C., Cheng, C. K., Huang, C. H., and Lo, W. H., 2001, "The Influence of Inserting a Fuji Pressure Sensitive Film Between the Tibiofemoral Joint of Knee Prosthesis on Actual Contact Characteristics," Clin. Biomech., **16**, pp. 160–166.
[33] Bachus, K. N., DeMarco, A. L., Judd, K. T., Horwitz, D. S., and Brodke, D. S., 2006, "Measuring Contact Area, Force, and Pressure for Bioengineering Applications: Using Fuji Film and TekScan Systems," Med. Eng. Phys., **28**, pp. 483–488.
[34] Fregly, B. J., and Sawyer, W. G., 2003, "Estimation of Discretization Errors in Contact Pressure Measurements," J. Biomech., **36**, pp. 609–613.
[35] Hoffmann, K. and Decker, K., 2008, "Inaccuracies in Measurement of Contact Pressure Due to the Measuring Grid of a Foil Sensor," Int. J. Intell. Syst. Technol. Appl., **3**, pp. 80–94.
[36] el-Bohy, A. A., Yang, K. H., and King, A. I., 1989, "Experimental Verification of Facet Load Transmission by Direct Measurement of Facet Lamina Contact Pressure," J. Biomech., **22**, pp. 931–941.
[37] Kettler, A., Rohlmann, F., Neidlinger-Wilke, C., Werner, K., Claes, L., and Wilke, H. J., 2006, "Validity and Interobserver Agreement of a New Radiographic Grading System for Intervertebral Disc Degeneration: Part II. Cervical Spine," Eur. Spine J., **15**(6), pp. 732–741.
[38] Frobin, W., Leivseth, G., Biggemann, M., and Brinckmann, P., 2002, "Vertebral Height, Disc Height, Posteroanterior Displacement and Dens-Atlas Gap in the Cervical Spine: Precision Measurement Protocol and Normal Data," Clin. Biomech., **17**(6), pp. 423–431.
[39] Kikkawa, J., Cunningham, B. W., Shirado, O., Hu, N., McAfee, P. C., and Oda, H., 2010, "Multidirectional Flexibility of the Spine Following Posterior Decompressive Surgery after Single-Level Cervical Disc Arthroplasty: An in Vitro Biomechanical Investigation," Spine, **35**(25), pp. E1465–E1471.
[40] Ehteshami, J., Natarajan, R., and An, H. S., 2010, "The Effects of Endplate Distraction During Cervical Spine Arthroplasty on Endplate Stress," 38th Annual Meeting of the Cervical Spine Research Society, Paper No. #71.
[41] Dunlop, R. B., Adams, M. A., and Hutton, W. C., 1984, "Disc Space Narrowing and the Lumbar Facet Joints," J. Bone Joint Surg. Br., **66**, pp. 706–710.
[42] Siegmund, G. P., Heinrichs, B. E., Lawrence, J. M., and Philippens, M. M., 2001, "Kinetic and Kinematic Responses of the RID2a, Hybrid III and Human Volunteers in Low-Speed Rear-End Collisions," Stapp Car Crash J., **45**, pp. 239–256.
[43] Walker, L. B., Harris, E. H., and Pontius, U. R., 1973, "Mass, Volume, Center of Mass and Mass Moment of Inertia of Head and Head and Neck of the Human Body," 17th Stapp Car Crash Conference, Paper No. #730985.
[44] Nuckley, D. J., Konodi, M. A., Raynak, G. C., Ching, R. P., and Mirza, S. K., 2002, "Neural Space Integrity of the Lower Cervical Spine: Effect of Normal Range of Motion," Spine, **27**(6), pp. 587–595.
[45] Yoganandan, N., Pintar, F. A., Zhang, J., and Baisden, J. L., 2009, "Physical Properties of the Human Head: Mass, Center of Gravity and Moment of Inertia," J. Biomech., **42**(9), pp. 1177–1192.
[46] Patwardhan, A. G., Havey, R. M., Ghanayem, A. J., Diener, H., Meade, K. P., Dunlap, B., and Hodges, S. D., 2000, "Load-Carrying Capacity of the Human

Cervical Spine in Compression is Increased Under a Follower Load," Spine, **25**(12), pp. 1548–1554.
[47] Puttlitz, C. M., Rousseau, M. A., Xu, Z., Hu, S., Tay, B. K., and Lotz, J. C., 2004, "Intervertebral Disc Replacement Maintains Cervical Spine Kinetics," Spine, **29**(24), pp. 2809–1814.
[48] Panjabi, M. M., 1992, "The Stabilizing System of the Spine. Part II. Neutral Zone and Instability Hypothesis," J. Spinal Disord., **5**, pp. 390–397.
[49] Goel, V. K. and Clausen, J. D., 1998, "Prediction of Load Sharing Among Spinal Components of a C5-C6 Motion Segment Using the Finite Element Approach," Spine, **23**, pp. 684–691.
[50] Schendel, M. J., Wood, K. B., Buttermann, G. R., Lewis, J. L., and Ogilvie, J. W., 1993, "Experimental Measurement of Ligament Force, Facet Force, and Segment Motion in the Human Lumbar Spine," J. Biomech., **26**, pp. 427–438.
[51] Teo, E. C., and Ng, H. W., 2001, "Evaluation of the Role of Ligaments, Facets and Disc Nucleus in Lower Cervical Spine Under Compression and Sagittal Moments Using Finite Element Method," Med. Eng. Phys., **23**, pp. 155–164.
[52] Panjabi, M. M., Crisco, J. J., Vasavada, A., Oda, T., Cholewicki, J., Nibu, K., and Shin, E., 2001, "Mechanical Properties of the Human Cervical Spine as Shown by Three-Dimensional Load-Displacement Curves," Spine, **26**, pp. 2692–2700.
[53] White, A. A., and Panjabi, M. M., 1990, *Clinical Biomechanics of the Spine*, Lippincott, Philadelphia.
[54] Cholewicki, J., Panjabi, M. M., Nibu, K., and Macias, M. E., 1997, "Spinal Ligament Transducer Based on a Hall Effect Sensor," J. Biomech., **30**, pp. 291–293.
[55] Stemper, B. D., Yoganandan, N., and Pintar, F. A., 2005, "Effects of Abnormal Posture on Capsular Ligament Elongations in a Computational Model Subjected to Whiplash Loading," J. Biomech., **38**, pp. 1313–1323.
[56] Yamamoto, I., Panjabi, M. M., Crisco, T., and Oxland, T., 1989, "Three-Dimensional Movements of the Whole Lumbar Spine and Lumbosacral Joint," Spine, **14**, pp. 1256–1260.
[57] Cook, D. J., and Cheng, B. C., 2010, "Development of a Model Based Method for Investigating Facet Articulation," J. Biomech. Eng., **132**(6), p. 064504.
[58] Serhan, H. A., Varnavas, G., Dooris, A. P., Patwadhan, A., and Tzermiadianos, M., 2007, "Biomechanics of the Posterior Lumbar Articulating Elements," Neurosurg. Focus, **22**, pp. E1.
[59] Haher, T. R., O'Brien, M., Dryer, J. W., Nucci, R., Zipnick, R., and Leone, D. J., 1994, "The Role of the Lumbar Facet Joints in Spinal Stability. Identification of Alternative Paths of Loading," Spine **19**, pp. 2667–2671.
[60] Murtagh, R. D., Quencer, R. M., Cohen, D. S., Yue, J. J., and Sklar, E. L., 2009, "Normal and Abnormal Imaging Findings in Lumbar Total Disk Replacement: Devices and Complications," Radiographics, **29**, pp. 105–118.
[61] Lemaire, J. P., Carrier, H., Sariali el, H., Skalli, W., and Lavaste, F., 2005, "Clinical and Radiological Outcomes With the Charite Artificial Disc: a 10-Year Minimum Follow-Up," J. Spinal Disord. Tech., **18**, pp. 353–359.
[62] van Ooij, A., Oner, F. C., and Verbout, A. J., 2003, "Complications of Artificial Disc Replacement: A Report of 27 Patients With the SB Charite Disc," J. Spinal Disord. Tech., **16**, pp. 369–383.